

Biomaterials Science: Processing, Properties, and Applications

Edited by
Roger Narayan
Amit Bandyopadhyay
Susmita Bose

C*eramic*
*T**ransactions*
Volume 228

 **WILEY**



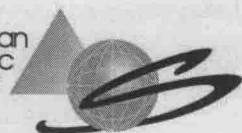
Biomaterials Science— Processing, Properties, and Applications

Ceramic Transactions, Volume 228

Edited by
Roger Narayan
Amit Bandyopadhyay
Susmita Bose



The
American
Ceramic
Society



 **WILEY**

A John Wiley & Sons, Inc., Publication

Copyright © 2011 by The American Ceramic Society. All rights reserved.

Published by John Wiley & Sons, Inc., Hoboken, New Jersey.
Published simultaneously in Canada.

No part of this publication may be reproduced, stored in a retrieval system, or transmitted in any form or by any means, electronic, mechanical, photocopying, recording, scanning, or otherwise, except as permitted under Section 107 or 108 of the 1976 United States Copyright Act, without either the prior written permission of the Publisher, or authorization through payment of the appropriate per-copy fee to the Copyright Clearance Center, Inc., 222 Rosewood Drive, Danvers, MA 01923, (978) 750-8400, fax (978) 750-4470, or on the web at www.copyright.com. Requests to the Publisher for permission should be addressed to the Permissions Department, John Wiley & Sons, Inc., 111 River Street, Hoboken, NJ 07030, (201) 748-6011, fax (201) 748-6008, or online at <http://www.wiley.com/go/permission>.

Limit of Liability/Disclaimer of Warranty: While the publisher and author have used their best efforts in preparing this book, they make no representations or warranties with respect to the accuracy or completeness of the contents of this book and specifically disclaim any implied warranties of merchantability or fitness for a particular purpose. No warranty may be created or extended by sales representatives or written sales materials. The advice and strategies contained herein may not be suitable for your situation. You should consult with a professional where appropriate. Neither the publisher nor author shall be liable for any loss of profit or any other commercial damages, including but not limited to special, incidental, consequential, or other damages.

For general information on our other products and services or for technical support, please contact our Customer Care Department within the United States at (800) 762-2974, outside the United States at (317) 572-3993 or fax (317) 572-4002.

Wiley also publishes its books in a variety of electronic formats. Some content that appears in print may not be available in electronic formats. For more information about Wiley products, visit our web site at www.wiley.com.

Library of Congress Cataloging-in-Publication Data is available.

ISBN: 978-1-118-06001-8
ISSN: 1042-1122

oBook ISBN: 978-1-118-14456-5
ePDF ISBN: 978-1-118-14453-4

Printed in the United States of America.

10 9 8 7 6 5 4 3 2 1

Biomaterials Science— Processing, Properties, and Applications

Second Edition, Volume 246

Edited by

Roger Narayan

André D. Jenkins

Shirley A. Barlow

WILEY

A JOHN WILEY & SONS PUBLICATION

Preface

This volume is a collection of eighteen research papers from the symposia on Next Generation Biomaterials and Surface Properties of Biomaterials, held during the 2010 Materials Science & Technology Conference & Exhibition (MS&T'10), Houston, TX, October 17–22, 2010.

These symposia focused on several key areas, including biomaterials for tissue engineering, ceramic biomaterials, metallic biomaterials, biomaterials for drug delivery, nano-biomaterials, biocompatible coatings, and surface modifications.

We would like to thank the following symposium organizers for their valuable assistance: Suwan Jayasinghe, University College London; Kalpana Katti, North Dakota State University; Kajal Mallick, University of Warwick; Christopher Berndt, SUNY- Stony Brook; Devesh Misra, University of Louisiana, Paul Calvert, University of Massachusetts, and Mukesh Kumar, Biomet Inc. Thanks also to all of the authors, participants, and reviewers of this Ceramic Transactions proceedings issue.

We hope that this issue becomes a useful resource in the area of bioceramics research that not only contributes to the overall advancement of this field but also signifies the growing roles of The American Ceramic Society and its partner materials societies in this rapidly developing field.

ROGER NARAYAN, *University of North Carolina at Chapel Hill*
AMIT BANDYOPADHYAY, *Washington State University*
SUSMITA BOSE, *Washington State University*

Contents

Preface	vii
---------	-----

NEXT GENERATION BIOMATERIALS

Ultrafine-Grained Commercially Pure Titanium and Microstructure Response to Hydroxyapatite Coating Methods Kayla Calvert, Kevin Trumble, Srinivasan Chandrasekar, and Mark Hoffman	3
Preparation of Porous Hydroxyapatite Scaffolds using Yeast as a Pore Forming Agent Sophie C. Cox and Kajal K. Mallick	15
Understanding the Influence of SrO Doping on the Mechanical Properties of β -TCP Ceramics Ken DeVoe, Amit Bandyopadhyay, and Susmita Bose	27
Dental Application Field Based on Nanostructural Chemically Bonded Ca-Aluminate Leif Hermansson	33
Freeze Extrusion Fabrication of 13-93 Bioactive Glass Scaffolds for Repair and Regeneration of Load-Bearing Bones T. S. Huang, M. N. Rahaman, N. D. Doiphode, M. C. Leu, B. S. Bal, D. E. Day, and X. Liu	45
Porous Biodegradable Scaffolds for Hard Tissue Engineering Kajal K. Mallick and James Winnett	57

Synthesis of Nano Hydroxyapatite by Chemical Precipitation Using Different Surfactant Templates Shahid Amin and Mohammad Mujahid	67
Effect of TiB_2 or Y_2O_3 Additions on Mechanical Biofunctionality of Ti-29Nb-13Ta-4.6Zr for Biomedical Applications Mitsuo Niinomi, Masaaki Nakai, Satoshi Yonezawa, Xiu Song, and Lei Wang	75
Apatite Nano-Rods Array Grown on Glass Substrates in Aqueous Systems A. Osaka, Y. Shirosaki, S. Hayakawa, K. Tsuru, E. Fujii, and K. Kawabata	83
Dielectric Properties of Porous Calcium Titanate ($CaTiO_3$) G. A. Rott, F. Zhang, Y. Haba, W. Kröger, and E. Burkel	89
Nanocomposites of Poly(L-Lactic Acid) and Maghemite for Drug Delivery of Caffeine A. Vargas, F. G. Souza Jr.	95
SURFACE PROPERTIES OF BIOMATERIALS	
Hard and Wear Resistant Surfaces for Load Bearing Metal Implants Vamsi Krishna Balla, Susmita Bose, and Amit Bandyopadhyay	109
Influence of Electro-Thermal Polarization on Surface Properties of Hydroxyapatite S. Bodhak, S. Bose, and A. Bandyopadhyay	125
Calcium Phosphate Ceramics in Drug Delivery and Bone Tissue Engineering Susmita Bose, Solaiman Tarafder, Shashwat Banerjee, and Amit Bandyopadhyay	135
Nanoscale Hydroxyapatite Coatings on Ti: Simultaneous Enhancement of Mechanical and Biological Properties Mangal Roy, Amit Bandyopadhyay, and Susmita Bose	147
Thermal Sprayed Bioceramics Coatings for Metallic Implants T. P. S. Sarao, H. Singh, H. Singh, and R. Chhibbe	159
Role of Reinforced Materials in Thermal Sprayed Hydroxyapatite Coating on Bio Implants: A Review Gurbhinder Singh, Surendra Singh, and Satya Prakash	173
Selective Laser Sintering Fabrication of 13-93 Bioactive Glass Bone Scaffolds M. Velez, K. C. R. Kolan, M. C. Leu, G. E. Hilmas, and R. F. Brown	185
Author Index	195

ULTRAFINE-GRAINED COMMERCIALLY PURE TITANIUM AND MICROSTRUCTURE RESPONSE TO HYDROXYAPATITE COATING METHODS

Kayla Calvert¹, Kevin Trumble¹, Srinivasan Chandrasekar² and Mark Hoffman³

¹School of Materials Engineering, ²School of Industrial Engineering at Purdue University, West Lafayette, IN, USA and ³School of Materials Science and Engineering at University of New South Wales, Sydney, Australia

ABSTRACT

Hydroxyapatite coating of orthopaedic implant materials generally involves high temperature plasma spray, which can initiate recrystallization and/or grain growth in ultrafine-grained (UFG) titanium. Therefore, two alternative low-temperature hydroxyapatite coating methods (sol-gel spin coating followed by calcination (325-450°C) and anodization followed by hydrothermal processing (200-225°C)) are also investigated in terms of coating quality and thermal stability of the UFG titanium substrate. Plasma spray produced a crystalline coating ~38 µm thick with essentially no influence on the UFG titanium substrate. Sol-gel coating followed by calcination resulted in highly variable coatings with recrystallization and grain growth in the ultrafine grained titanium substrate. Anodization followed by a controlled hydrothermal process resulted in a homogeneous, roughened and porous coating integrating Ca and P ions into the Ti substrate. This work presents a unique hydrothermal processing route for conversion of the anodized precursor film. The underlying UFG Ti substrate was not influenced by the hydrothermal processing.

INTRODUCTION

Commercially pure titanium (cp-Ti) is an ideal biomaterial as it does not invoke a local or systemic response in the body. However, in orthopaedic applications Ti alloys are commonly implanted due to higher strength compared to cp-Ti. Thus, strengthening cp-Ti without alloying is attractive for orthopaedic applications. Ultrafine-grained (UFG) cp-Ti (ASTM grade 2) has been developed using a single-step deformation route via machining [1]. Compared to annealed grade 2-Ti, the grain size was reduced from ~34 µm to ~100 nm with a hardness increase of ~40% in the machined UFG-Ti [1].

Non-cemented orthopaedic devices are commonly coated with hydroxyapatite (HA), $\text{Ca}_{10}[\text{PO}_4]_6[\text{OH}]_2$, to promote osteointegration of the implant. The stoichiometric ratio of Ca and P in hydroxyapatite is 1.67; however, the measured value is commonly reported between 1.5 and 1.7. Major orthopaedic companies including Stryker, Smith and Nephew, DePuy, Biomet and Zimmer use HA applied via plasma spray [2]. In the commercialized process, HA powder in a plasma jet (temperatures exceeding 10,000°C) becomes molten and is blasted onto the substrate surface. The thickness of this HA layer is commonly between 50 and 200 µm [2] depending on the processing parameters. Although the HA plasma spray has an established precedent in the orthopaedic community, the process may not be suitable for UFG-Ti. The machining process is a severe plastic deformation (SPD) process that induces a large amount of shear strain, which is accommodated by dislocations. The high dislocation density of the UFG microstructure lowers the thermal stability compared to conventional grain sized titanium and recrystallization occurs at temperatures between 300 and 400°C in machined ultrafine grained titanium [1]. Clearly, recrystallization and the associated loss of hardness and strength is undesirable in the UFG

microstructure, thus alternative low-temperature HA processing routes must be investigated in terms of their influence on the thermal stability of UFG-Ti.

In a processing route first developed by Ishizawa et al. [3-5], anodization of a Ti substrate in a solution containing Ca and P ions followed by a hydrothermal treatment in high pressure steam at 300°C for 2 h developed a layer with Ca and P ions. The analysis of these layers revealed the integration with the Ti substrate and development of HA rich zones. Alternatively, Liu et al. [6] showed that a sol-gel precursor applied by dip coating and followed by calcination at temperatures as low as 350°C results in the apatitic phase of a homogeneous HA layer.

In this work, plasma spray as well as two alternative low-temperature methods (sol-gel spin-coating followed by calcination and anodization followed by hydrothermal processing) will be investigated. The purpose of this study is twofold: 1) to characterize the developed coatings and 2) to evaluate the thermal response of the UFG-Ti substrate to the HA coating processes.

MATERIALS & METHODS

The UFG-Ti substrates were produced in the form of strips 5 mm wide x 0.2 mm thick using ASTM commercially pure grade 2-Ti (McMaster-Carr) in a machining process with imposed shear strains (γ) of ~2.0 to 3.4, as detailed elsewhere [1]. The HA coatings were applied using three different methods: (1) commercial plasma spray, (2) anodization with hydrothermal processing and (3) spin coating of a sol-gel followed by calcination.

Hydroxyapatite Processing

In the commercial plasma spray by ASDM (Sydney, Australia) the surface was grit blasted with Al_2O_3 prior to HA spray, enhancing surface roughness and HA adherence. HA plasma spray conditions for the UFG-Ti substrates were not disclosed.

Following the sol-gel method described by Liu et al. [6], a viscous sol with a Ca/P ratio of 1.67 was developed by mixing 3 M triethyl phosphite (stirred for 20 minutes to allow for hydrolyzation of the phosphite) and 2 M calcium nitrate. After aging at room temperature for 18 h, the sol was heated at 60°C for 1 h to produce the gel. The surface of the UFG-Ti strip was covered with the sol-gel compound and spun at 2000 RPM for 45 s. Eight layers were applied to each substrate with an intermediate drying step of 30 min at 72°C after each layer was applied. After application of the sol-gel layers, the substrates were placed in a box furnace in air for 2 h at 325, 350 or 450°C (actual thermocouple measurement 313, 339, 446°C) for calcination of the HA.

For anodization, the method described by Ishizawa et al. was followed [3-5]. UFG-Ti substrates (1 cm x 0.5 cm) were exposed to a high voltage in an aqueous solution containing Ca and P ions to produce a precursor HA film. Two solutions, 0.04 M β -glycerophosphate (β -GP, Alfa-Aesar, sodium beta-glycerophosphate pentahydrate) and 0.25 M calcium acetate (CA, Sigma Aldrich, calcium acetate monohydrate, 99+% ACS reagent), were mixed together to form a Ca/P stoichiometric ratio of 1.67, as in HA. The substrates were attached to a conductive brass strip with masking tape and a voltage was applied. The ideal current density for anodization is 50 mA/cm² [3-5], which corresponded to 25 mA for the Ti substrates. The maximum current measured was 10 mA and voltage was 350 V in this experiment. Although the ideal current density was not obtained, the voltage range (300 to 350 V) was similar to that applied by Ishizawa et al. [3-5]. The voltage was applied for 1 to 5 min. After anodization, a hydrothermal process was developed for the conversion of Ca and P to crystalline HA. The hydrothermal conversion was carried out in an acid digestion bomb (Parr Instruments Company, 302 AC-

T304) with a 125 mL polytetrafluoroethylene liner. Previous work has indicated that Ca and P ions can leach out in solution during a hydrothermal treatment when Ca and P ions are not contained in the solution [7]. Therefore, the following hydrothermal treatments were performed: 225 °C in H₂O for 4 or 20 h as well as 200 °C in solution of 5.7×10^{-4} M Ca²⁺ with 3.3×10^{-4} M PO₄³⁻ ions (pH of 11) for 20 h followed by 225 °C in H₂O for 20 h. The Ca and P solution used during the hydrothermal process was made by mixing 0.04 g of CA and 0.02 g of KH₂PO₄ (Sigma, Potassium phosphate mono ACS reagent ≥99.0%) in 44.5 mL of sodium hydroxide.

Coating Characterization

Optical microscopy was used for thickness evaluation of the HA layers. However, the sol-gel calcined layer was not resolved in light microscopy, thus cross-sections were milled from the substrates using a focused ion beam (FIB) (FEI, Model xP200) and imaged with TEM (JEOL, Model 1400) in a process described elsewhere [1]. Further characterization of the anodized and plasma sprayed samples was conducted using SEM (JEOL, T3000) with EDS. As the sol-gel layer was too thin for SEM chemical analysis, TEM chemical analysis with EDAX was utilized. X-ray diffraction (Bruker, D8 Focus) with CuKα was used to evaluate the crystallinity of the layer developed in the anodized and hydrothermally treated layer.

Substrate Characterization

To evaluate the thermal stability of the UFG-Ti substrate, both microstructural analysis and Vickers hardness were examined before and after application of the HA. For microstructural analysis, optical microscopy as well as TEM was used for grain size evaluation. In optical microscopy, coated UFG-Ti was mounted in Bakelite, polished and etched with Kroll's reagent to reveal the grain microstructure. For TEM imaging, FIB was again employed to lift out small (10 μm x 2 μm x 100 nm) cross-sections of the Ti substrate. The Vickers microhardness (Leco, Model LM247AT) was measured along the cross-section of the UFG-Ti substrate with at least fifteen measurements per sample. The indents were made at least three indent spacings away from the edges and other indents with a load of 0.2 kgf.

RESULTS AND DISCUSSION

The grain size of conventional grain grade 2-Ti was 34 ± 5 μm, while the grain size of the as-machined grade 2-Ti was ~100 nm [1]. The microhardness of the conventional grain grade 2-Ti was 188 ± 7 HV, while the as-machined UFG-Ti exhibited a hardness of 246 ± 7 HV independent of shear strain in the range of $\gamma \sim 2.3$ to 3.4. In addition, for reference, a TEM image the as-machined UFG-Ti microstructure is shown in Figure 1.

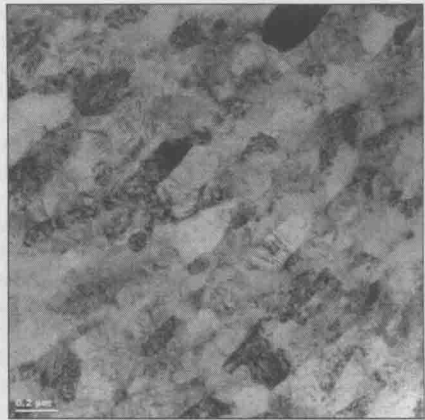


Figure 1: Bright-field TEM image of uncoated UFG-Ti with $\gamma \sim 3.4$.

Plasma Spray

As shown in Figure 2a, the HA plasma sprayed layer reveals an elongated microstructure with mechanical locking on the Ti substrate. The elongated structure is expected from the molten plasma hitting and spreading across the surface. Processing parameters were not disclosed by ASDM; however the process produced a HA layer with an average thickness of $38 \pm 11 \mu\text{m}$ and a range of 20 to 70 μm . From EDS, the average atomic Ca/P ratio was 1.81, which is slightly higher than the reported HA range. Figure 2b shows the Ti substrate after plasma spray, and there appears to be no change in the microstructure. Flow lines, as exhibited in the as-machined UFG-Ti, [1] are clearly observed from the visible subgrains. The microstructural analysis suggests that the thermal processing during plasma spray does not affect the UFG-Ti substrate. Furthermore, the microhardness of the plasma sprayed UFG-Ti with $\gamma \sim 2.3$ was $244 \pm 7 \text{ HV}$ and showed no significant difference (student t-test, p-value = 0.928) from the as-machined UFG-Ti. These results suggest that although plasma spray is a high temperature process, the UFG microstructure is unaffected, possibly due to substrate cooling during the process or the very low heat capacity of the HA plasma.

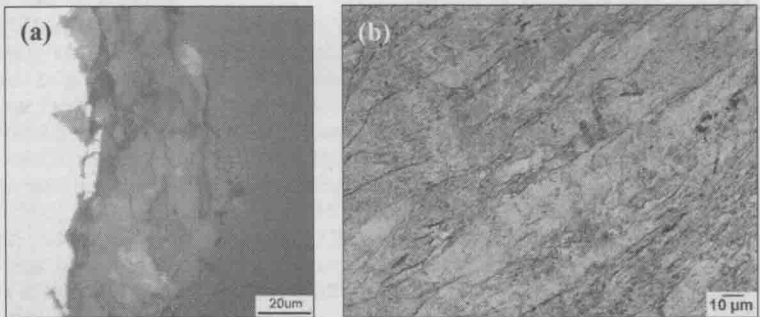


Figure 2: Light microscopy images of (a) HA sprayed layer on UFG-Ti and (b) UFG-Ti substrate with $\gamma \sim 2.3$ after HA plasma spray.

Sol-Gel Coating

From TEM analysis, the thickness of the calcined sol-gel layer produced at 339°C (Figure 3) and 446°C was observed to be highly variable. Along the same TEM sample, the layer was very thin and not visible in some areas and ~500 nm in other areas. The average thickness was 150 – 175 nm for calcinations at 313°C and 446°C. In addition to the highly variable layer thickness, EDAX revealed a separation of calcium and phosphorous rich regions. Thus, the sol-gel method followed by calcinations did not produce crystalline HA. These results do not follow those reported by Kim et al., in which dip coating of the sol-gel resulted in a 1 μm crystalline HA layer with a Ca/P ratio between 1.61 and 1.72 [8].

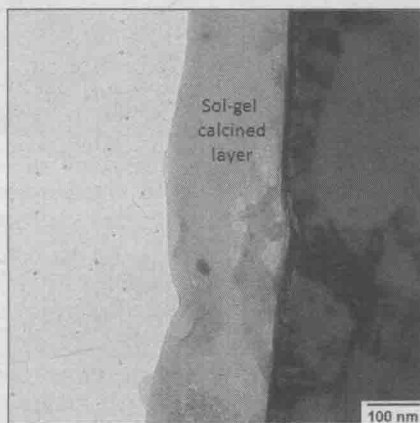


Figure 3: Bright-field TEM image of sol-gel calcined layer at 313°C on UFG-Ti with $\gamma \sim 3.4$.

Figures 4a and 4b show the Ti substrate after sol-gel coating and calcination at 313°C and 446°C, respectively. As shown, significant microstructural changes of the as-machined UFG-Ti have occurred compared to the TEM image in Figure 1. After the calcination, distinct grains are evident with equiaxed grains dominating the microstructure. Grain growth is clear between Figures 4a and 4b as the grains are ~170 nm from calcination at 313°C and ~340 nm from calcination at 446°C.

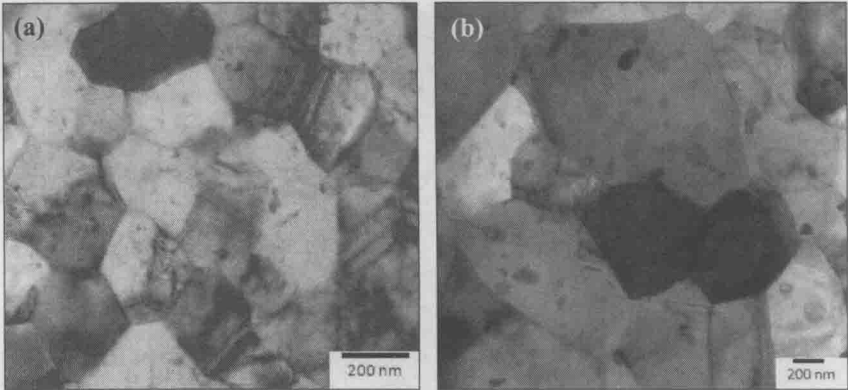


Figure 4: Bright-field TEM images from sol-gel calcined UFG-Ti substrates at (a) 313°C and (b) 446°C.

Furthermore, the microhardness values of the calcined substrates are lower than the as-machined condition, as shown in Table I. Thus, it is clear that significant microstructural changes affect the mechanical properties of the UFG-Ti through this HA application route. Based on variability in the HA layer produced, as well as the significant changes in the substrate, this sol-gel coating and calcination is not a viable low-temperature coating process for UFG-Ti substrates.

Table I. Vickers microhardness of sol-gel coated and calcined UFG-Ti substrates with $\gamma \sim 3.4$.

Calcination Temp (°C)	Hardness (HV)
313	240 ± 8
339	234 ± 7
446	215 ± 3

Anodized with Hydrothermal Processing

Anodization followed by hydrothermal treatment produced homogenous layers with thicknesses between 5 and 15 μm depending on the applied voltage. For anodization at 350 V, the thickness was $10 \pm 3 \mu\text{m}$, which is consistent with previous reports for anodized Ti. Ishizawa and Ogino [5] reported a thickness of $\sim 10 \mu\text{m}$ for anodization at 350 V, while Zhu, Kim and Jeong [9] reported thicknesses between 5 and 7 μm at 350 V.

Figure 5 shows an SEI-SEM plan view image of the anodized surface prior to hydrothermal conversion. In the anodization process, Ca and P ions are chemically bound to the newly formed titanium oxide, and EDS revealed that the average Ca/P atomic ratio was 0.92 with Ti as the major constituent ($\sim 75 \text{ wt\%}$). This confirms that Ca and P ions are integrated with the anodized Ti, as the electron interaction volume in SEI-SEM is only $\sim 1\text{-}2 \mu\text{m}$. In addition, the “ring” structure is beneficial for orthopaedics, as rough and porous surfaces are known to enhance osteointegration [10]. Although the Ca/P ratio was 0.92 for the anodized surface, a higher concentration of $\beta\text{-GP}$ will increase the Ca/P ratio [5].

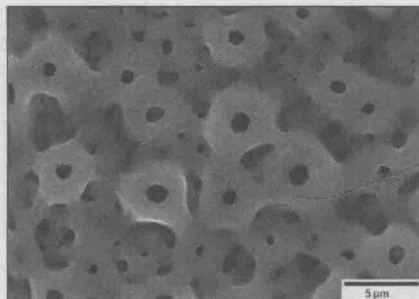


Figure 5: SEI-SEM plan view image of anodized UFG-Ti surface.

Figure 6a shows an SEI-SEM plan view image of the anodized surface after hydrothermal conversion in H_2O for 4 h at $225^\circ C$. The white regions are HA rich (~ 45 wt% Ti of the elements detected) while the material surrounding the pores is Ti rich (~ 94 wt% Ti). Although HA rich regions are formed, they are inhomogeneous, small (~ 4.5 μm) and not well integrated with the Ti. Therefore, the microstructure developed after 4 h in H_2O of hydrothermal processing is not ideal for orthopaedic applications. Figure 6b shows an SEI-SEM plan view image of the anodized surface after hydrothermal conversion in H_2O for 20 h at $225^\circ C$. Again, the white regions are HA rich (~ 8 to 15 wt% Ti of the elements detected) while the material surrounding the pores is Ti rich (~ 86 to 91 wt% Ti). As expected with a longer processing time under the same temperature and medium, coarsening of the HA rich zones occurs compared to the microstructure after 4 h. The HA rich regions are not integrated with the Ti substrate and are ~ 12 μm in width. The faceted HA rich regions have atomic Ca/P ratios in the range of 1.16 to 1.49, which is close to stoichiometric HA. Although the substrate exhibits more HA rich areas than at 4h, the coating is again inhomogeneous. Thus, hydrothermal processing in H_2O is not suitable for orthopaedic applications as the HA rich regions are not homogeneous and are not well integrated with the Ti substrate.

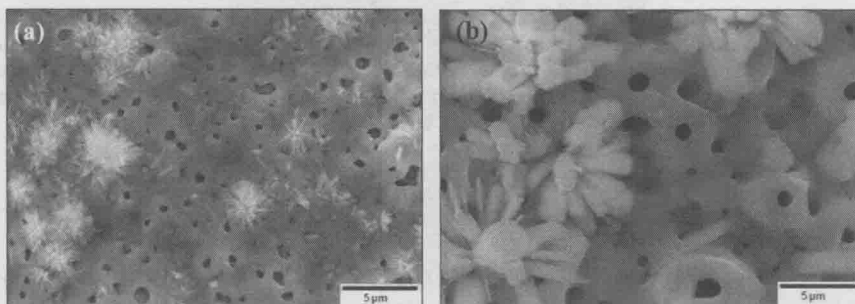


Figure 6: SEI-SEM plan view images of hydrothermal treatment in H_2O at (a) $225^\circ C$ for 4 h and (b) $225^\circ C$ for 20 h.

In an attempt to keep HA from nucleating inhomogeneously, the hydrothermal process was conducted in a medium of Ca and P ions. After hydrothermal treatment in a solution containing Ca and P ions, the substrate was subsequently hydrothermally treated in H_2O to

nucleate HA. The final processing route with two hydrothermal steps (20 h at 200°C in Ca and P solution followed by 20 h at 225°C in H₂O) resulted in the most homogenous HA rich zones surrounding the pores. As shown in Figure 7, no faceted HA crystals are observed and the HA appears to be well integrated with the Ti substrate. In addition, the roughened surface is advantageous in promoting osteointegration [10]. Around the pores the Ca/P atomic ratio was 1.58 with 81 wt% Ti of the elements detected, while away from the pores, the Ca/P ratio was 0.58 with 85 wt% Ti. The resulting XRD patterns from this hydrothermal process followed the JCPDS pattern #074-0566 [11] for crystalline HA ($\text{Ca}_{10}(\text{PO}_4)_6(\text{OH})_2$). As analyzed in XRD, neither the as-anodized Ti nor the hydrothermal treated substrates in H₂O alone result in crystalline HA.

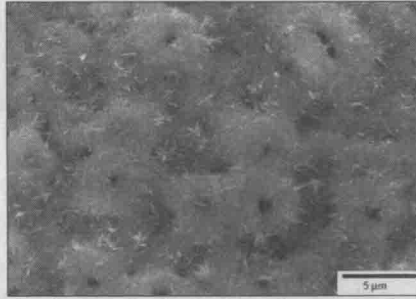


Figure 7: SEI-SEM plan view image after hydrothermal treatment for 20 h at 200°C in Ca and P solution followed by 20 h at 225°C in H₂O.

After hydrothermal treatment at the highest temperature (225°C) for 20h, the microstructure of the Ti substrate was imaged with light microscopy (Figure 8) and TEM (Figure 9). As shown in Figure 8, flow lines with subgrains are distinct as in the as-machined Ti. Furthermore, Figure 9 shows the subgrain microstructure that is intact after processing at 225°C for 20 h. These images suggest that no recovery or recrystallization occurs after hydrothermal processing. Additionally, the microhardness values of the Ti substrates after hydrothermal processing are shown in Table II. The hardness results for all hydrothermal treatments are not statistically different ($p > 0.05$) than the as-machined Ti. These results are consistent with an annealing study on the machined UFG-Ti [1]. Therefore, based on the microstructure and microhardness values, no change is initiated in UFG-Ti with hydrothermal processing at 200 – 225°C.